DOI: 10.1002/zaac.202400130

$La_{11}Si_{11}P_{21}Te_5$ and $La_{20.667}Si_{18}P_{46}Te_{11.333}$: Two Novel 3D-Polyanionic Lanthanum Compounds Following the Zintl-Klemm Concept

Patrik Djendjur,[a] Zoë A. Anschütz,[a] Rainer Niewa,[a] and Thomas Schleid*[a]

Dedicated to Professor Thomas Fässler on the Occasion of his 65th Birthday.

During attempts to synthesize La_3PTe_3, after participation of the SiO_2-container material, two so far unknown compounds could be isolated, which both follow the Zintl-Klemm concept. The novel quaternary lanthanum tellurides $La_{11}Si_{11}P_{21}Te_5$ and $La_{20.667}Si_{18}P_{46}Te_{11.333}$ crystallize hexagonally in the non-centrosymmetric space group $P\bar{6}2c$ with the unit-cell parameters $a = 1204.97(6)$ pm and $c = 1802.38(9)$ pm ($c/a = 1.496$) or $a = 1205.78(6)$ pm and $c = 1802.16(9)$ pm ($c/a = 1.495$), respectively. Their very similar crystal structures can be divided into two interpenetrating three-dimensional sublattices, $^3_\infty\{[La_{11}Te_5]^{23+}\}$ ($d(La^{3+}–Te^{2-}) = 314–335$ pm *plus* 352 pm) and $^3_\infty\{[Si_{11}P_{21}]^{23-}\}$ (d(Si–P) = 221–225 pm, d(Si–Si) = 230–231 pm, d(P–P) = 220–221 pm) for $La_{11}Si_{11}P_{21}Te_5$ ($Z = 2$), displaying unique structural features as compared to related compounds. The linkage of these two sublattices occurs through attractive $La^{3+}–Si^-$ and $La^{3+}–P^-$ interactions (d(La–Si) = 333 pm, d(La–P) = 298–318 pm). For $La_{20.667}Si_{18}P_{46}Te_{11.333}$ ($Z = 1$), $^4/_3$ out of 22 La^{3+} cations in the doubled formula $La_{22}Si_{22}P_{42}Te_{10}$ have to be omitted, while the four Si^- anions need to be replaced with phosphorus atoms. The La^{3+} vacancies are filled up with tellurium, partly forming $[Te_2]^{2-}$ dumbbells (d(Te–Te) = 274 pm). $La_{11}Si_{11}P_{21}Te_5$ can be obtained on target by reacting the elements (La, Si, P and Te) in their respective amounts with an excess of potassium chloride as fluxing agent in evacuated and torch-sealed glassy silica ampoules for four days at 900 °C as black pillars or thick plates with hexagonal cross-section.

Introduction

Sesquichalcogenides of the rare-earth metals RE_2Ch_3 (RE = La–Nd, Sm, Gd–Lu; Ch = S–Te) are known to exhibit multiple modifications, of which the C-type structure is the longest known.[1,2] In this cation-deficient Th_3P_4-type arrangement,[3,4,5] the rare-earth metal(III) cations are surrounded by eight chalcogenide anions, but need to be thinned out in a disordered manner, due to reasons of charge neutrality following the formula $(RE^{3+})_{2.667}\square_{0.333}(Ch^{2-})_4$ for $Z = 4$ ($\equiv RE_2Ch_3$ for $Z = 5.333$).[6] To compensate for the high cationic charge, it is possible to dope these compounds with phosphorus up to the point that all cationic positions can be filled, ending in the composition RE_3PCh_3.[7,8] It could be shown that this is easily possible for the lighter rare-earth metal compounds (RE = La–Nd, Sm) in the case of the lighter chalcogenides (Ch = S and Se). In an attempt to synthesize the tellurium analogues of these substances, instead of La_3PTe_3 in the lanthanum case the unexpected title compounds $La_{11}Si_{11}P_{21}Te_5$ and $La_{20.667}Si_{18}P_{46}Te_{11.333}$ could be isolated as single crystals and successfully characterized. The first one shows two distinct interpenetrating ionic networks $^3_\infty\{[La_{11}Te_5]^{23+}\}$ and $^3_\infty\{[Si_{11}P_{21}]^{23-}\}$, of which the anionic frame is built up from covalently bonded silicon and phosphorus atoms in a bonding situation best described by the Zintl-Klemm concept.[9–17] In this methodology, elements from the center of the periodic table, exhibiting an electron excess, show structural similarities to the elements of neighboring groups with the same valence electron number. In this example, the formal Si^- anions display features of phosphorus modifications (*e.g.* Na_4Si_4[18] with isolated $[Si_4]^{4-}$ tetrahedra mimicking white phosphorus P_4, Li_3NaSi_6[19] with a tube-like silicon structure just like in Hittorf's violet phosphorus) and the formal P^- anions exhibit properties, which can be found in sulfur or selenium modifications. One well-known example is the REPS (RE = Y, La–Nd, Sm, Gd–Tm)[20] substance class, where the phosphorus atoms form undulated infinite P–P chains, comparable to the ω-modification of sulfur[21] or gray selenium.[22]

The anionic $^3_\infty\{[Si_{11}P_{21}]^{23-}\}$ framework of title compound $La_{11}Si_{11}P_{21}Te_5$ shows great similarities to already known phosphidosilicates, of which a large variety is described in literature. This substance class typically comprises tetrahedral building blocks ($[SiP_4]^{8-}$ tetrahedra), which can appear isolated like in Li_8SiP_4[23,24] or $Li_4Sr_2SiP_4$,[25] condensed into strands like in Na_2SiP_2[26] and layers like in α-KSi_2P_3[27] or even into amazing

[a] P. Djendjur, Z. A. Anschütz, Prof. Dr. R. Niewa, Prof. Dr. Th. Schleid
Institute for Inorganic Chemistry
University of Stuttgart
Pfaffenwaldring 55
D-70569 Stuttgart (Germany)
Fax: +49-711-685-54239
E-mail: schleid@iac.uni-stuttgart.de

Supporting information for this article is available on the WWW under https://doi.org/10.1002/zaac.202400130 structural features such as Si–P supertetrahedra (Li_2SiP_2 and $LiSi_2P_3$[28] as well as β-KSi_2P_3[29]). The best examples for this class of compounds can be found in the Na–Si–P system (*e.g.* $NaSi_2P_3$, $Na_{19}Si_{13}P_{25}$ and $Na_{23}Si_{28}P_{45}$),[30] which do not only exhibit a wide variety of these structural supertetrahedral building blocks, but also demonstrate significant sodium-cation conductivity.[30] However, the diversity of bonding possibilities is even greater due to the relatively high tendency of silicon and phosphorus to form homoatomic bonds. By tuning the amount of the electron excess on the anionic sublattice, a plethora of bonding patterns can be achieved, so compounds with P–P and Si–Si bonds are described in the literature too. Interesting examples among them containing rare-earth metals originate from a short series with the empirical formula and $RESi_2P_6$ (RE = La–Nd),[31] where various phosphorus atoms through different numbers of homoatomic bonds cover oxidation states ranging from −3 to ±0 side by side in a single compound (*e.g.* $LaSi_2P_6$[32]). A rare example of a compound, in which P–P and Si–Si bonds occur simultaneously, is $Ba_3Si_4P_6$.[33] Here, an anionic sublattice of phosphorus and silicon atoms occurs, reminiscent of structural motifs known from Hittorf's phosphorus again.

A notable property of the title compound $La_{11}Si_{11}P_{21}Te_5$ is that, although various quaternary phosphidosilicates of the rare-earth elements are known, which predominantly exhibit an additional metallic component as extra cations, it contains extra anions, here Te^{2-} as well as Te^{2-} next to $[Te_2]^{2-}$ anions in $La_{20.667}Si_{18}P_{46}Te_{11.333}$. So, the two compounds we aim to present in this work demonstrate anionic derivatization instead and, in this light, represent a rarity in their field.

Results and Discussion

Source of Material

In an attempt to synthesize the ternary lanthanum phosphide telluride La_3PTe_3 in analogy to La_3PS_3 and La_3PSe_3,[7] a side reaction of the reactants (La, P and Te) with the glassy silica-ampoule material (SiO_2) occurred to form black single crystals of the so far unknown quaternary P- and Si-containing lanthanum telluride $La_{20.667}Si_{18}P_{46}Te_{11.333}$ (see Experimental Section). After having gained information about the rough composition, it was possible to prepare $La_{11}Si_{11}P_{21}Te_5$ on target by reacting its elemental components (La, Si, P and Te) in appropriate molar ratios from fused silica tubes using potassium chloride (KCl) as fluxing agent (see Experimental Section). The black pillars or thick plates with hexagonal cross-section (Figure 1) nicely reflect the crystal system, since these two novel lanthanum compounds crystallize hexagonally in the non-centrosymmetric space group $P\bar{6}2c$ containing two formula units per unit cell with the lattice parameters a = 1204.97(6) pm and c = 1802.38(9) pm for $La_{11}Si_{11}P_{21}Te_5$ from single-crystal X-ray diffraction (SCXRD) data. The crystallographic data of their mostly equivalent crystal structures are listed in Table 1. Rietveld refinements on powder X-ray diffraction (PXRD) data (a = 1204.9(1) pm and c = 1803.2(2) pm, see Experimental Section) could verify the unit-cell parameters from the single-crystal diffraction experiments. However, the composition of the firstly obtained crystals by serendipity differed slightly from that of the synthesis-on-target prepared ones. So, Table 1 not only shows the data for $La_{11}Si_{11}P_{21}Te_5$ (Z = 2) with its true composition, but also those for what turned out to be $La_{20.667}Si_{18}P_{46}Te_{11.333}$ (Z = 1) without significantly altered lattice constants (a = 1205.78(6) pm and c = 1802.16(9) pm). The occupation patterns of the Wyckoff positions for the individual atoms of both compounds are summarized in Tables 2 and 3.

Structure Description

In order to describe the two very similar crystal structures of both title compounds more precisely, it is easier to first divide them into the sublattices $\{[La_{11}Te_5]^{23+}\}$ and $\{[Si_{11}P_{21}]^{23-}\}$ for the $La_{11}Si_{11}P_{21}Te_5$ case. In the cationic sublattice $\{[La_{11}Te_5]^{23+}\}$, three distinct crystallographic tellurium positions are present, which all carry a double-negative charge. This comes a little surprising,

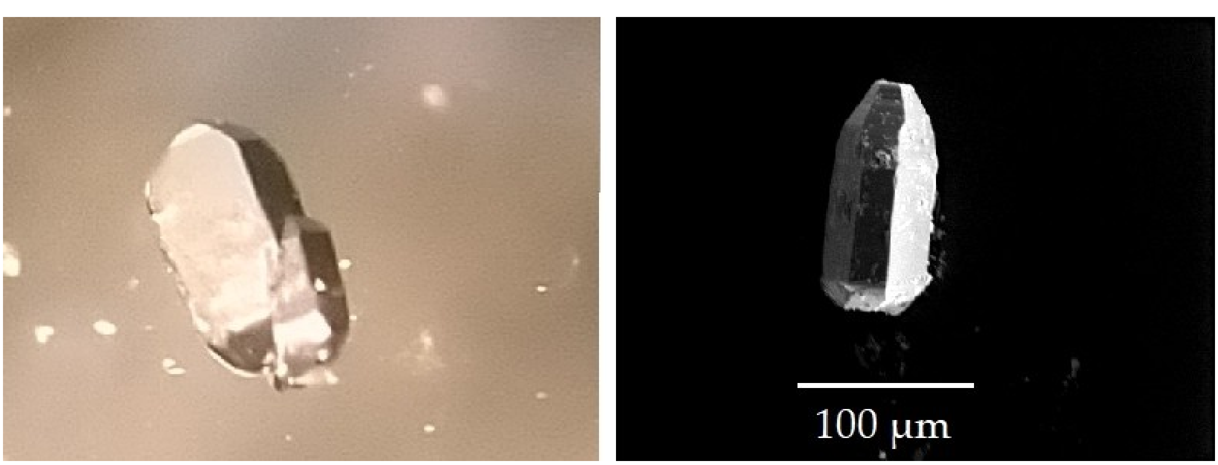

Figure 1. Black crystals of $La_{11}Si_{11}P_{21}Te_5$ as hexagonal pillars (light-microscopic (left) and back-scattered electron-microscopic pictures (right) with about the same scale).

Journal of Inorganic and General Chemistry
ZAAC
Zeitschrift für anorganische und allgemeine Chemie

Table 1. Crystallographic data for $La_{11}Si_{11}P_{21}Te_5$ (left) and $La_{20.667}Si_{18}P_{46}Te_{11.333}$ (right).

Empirical formula		$La_{11}Si_{11}P_{21}Te_5$	$La_{20.667}Si_{18}P_{46}Te_{11.333}$
Crystal system		hexagonal	
Space group		$P\bar{6}2c$ (no. 190)	
Lattice parameters,	a/pm	1204.97(6)	1205.78(6)
	c/pm	1802.38(9)	1802.16(9)
	c/a	1.496	1.495
Number of formula units, Z		2	1
Molar volume, V_m/cm^3·mol^{-1}		682.42(6)	1366.5(1)
Calculated density, D_x/g·cm^{-3}		4.580	4.572
Theta range, $2\theta_{max}$/°		54.96	64.07
Index range, $\pm h_{max}$ / $\pm k_{max}$ / $\pm l_{max}$		15 / 15 / 23	17 / 17 / 26
Electron sum, $F(000)$/e$^-$		2712	2709
Absorption coefficient, μ/mm^{-1}		14.32	14.13
Extinction coefficient, g/10^{-4}		12.2(11)	3.4(7)
Reflections (all / unique)		34575 / 1802	45856 / 2717
R_{int} / R_σ		0.094 / 0.040	0.074 / 0.030
Goodness-of-Fit		1.026	1.068
R_1 for all reflections		0.065	0.054
wR_2 for all reflections		0.124	0.116
Flack-x parameter[34]		−0.03(5)	0.00(3)
Residual electron density, ρ/e$^-$ 10^{-6} pm^{-3} (max. / min.)		3.32 / −3.45	3.16 / −3.23
CSD number		2361622	2351980

Table 2. Fractional atomic coordinates and equivalent isotropic displacement parameters for $La_{11}Si_{11}P_{21}Te_5$.

Atom	Wyckoff Site	Symmetry	x/a	y/b	z/c	U_{eq}/pm^2
La1	4*f*	3..	$^2/_3$	$^1/_3$	0.13243(9)	288(4)
La2	6*h*	*m*..	0.08464(13)	0.49941(13)	$^1/_4$	318(5)
La3	12*i*	1	0.24444(9)	0.16190(9)	0.13222(5)	256(3)
Si1	4*f*	3..	$^1/_3$	$^2/_3$	0.1382(3)	133(13)
Si2	6*g*	.2.	0.4548(5)	0	0	168(11)
Si3	12*i*	1	0.2607(4)	0.4682(4)	0.0848(2)	172(8)
P1	6*h*	*m*..	0.2315(5)	0.3521(5)	$^1/_4$	186(11)
P2	12*i*	1	0.4464(4)	0.1778(4)	0.0274(2)	182(8)
P3	12*i*	1	0.4305(4)	0.4443(4)	0.1011(2)	191(8)
P4	12*i*	1	0.1063(4)	0.3110(4)	0.1527(2)	176(7)
Te1	2*a*	32.	0	0	0	319(6)
Te2	2*b*	$\bar{6}$	0	0	$^1/_4$	188(5)
Te3	6*h*	*m*..	0.44747(19)	0.19091(19)	$^1/_4$	446(5)

since the sequence of electronegativies of the four components reads as follows: La (1.1 or 1.09), Si (1.9 or 1.74), Te (2.1 or 2.01) and P (2.2 or 2.06), when the first numbers represent the Pauling[35,36] and the second ones the Allred-Rochow scale.[37] Despite the higher values of phosphorus as compared to tellurium,[38a] the latter takes all valence electrons from lanthanum to complete its xenon shell. $(Te1)^{2-}$ and $(Te2)^{2-}$ are surrounded by six La^{3+} cations each (Figure 2, top). $(Te1)^{2-}$ shows a *pseudo*-octahedral or trigonal hemiprismatic (d(Te1–La3) = 351.5 pm, 6×) and $(Te2)^{2-}$ a real trigonal prismatic coordination environment (d(Te2–La3) = 335.7 pm, 6×). These polyhedra are linked via common triangular faces to form infinite columns $^1_\infty\{[Te1(La3)^f_{6/2}Te2(La3)^f_{6/2}]^{16+}\}$ (f = face-sharing) along the [001] direction. $(Te3)^{2-}$ is surrounded by only five La^{3+} cations in a square pyramidal shape (d(Te3–La) = 313.6–325.4 pm, see Table 4 for the individual values) and builds a propeller-like arrangement by sharing a common edge with two other square $[(Te3)La_5]^{13+}$ pyramids (Figure 2, bottom). Those columns all together form the three-dimensional cationic framework $^3_\infty\{[La_{11}Te_5]^{23+}\}$ as one sublattice of the $La_{11}Si_{11}P_{21}Te_5$ structure (Figure 3).

Lanthanum is located at three different crystallographic positions (Figure 4), in one of which $(La1)^{3+}$ exhibits the rather low coordination number of $C.N.$ = 6, being surrounded trigonal prismatically by three Te^{2-} anions and three phosphorus atoms (d(La1–P2) = 302.8 pm, 3×; d(La1–Te3) = 314.3 pm, 3×). The second La^{3+} position shows a rather high U_{eq} value with an inhomogeneous U_{ij} distribution (U_{11} = 429(9), U_{22} = 373(8), U_{33} = 164(6) pm^2) torn between the electronic lone pairs of the two $(Si1)^-$ anions and the $(Te3)^{2-}$ anion in its close vicinity, since $(La2)^{3+}$ is surrounded ninefold in a tricapped trigonal prismatic fashion by six phosphorus atoms alongside one Te^{2-} and two Si^- anions (d(La2–P) = 298.1–307.0 pm, 6×; see Table 4 for the individual values; d(La2–Te3) = 314.2 pm, 1×; d(La2–Si1) =

Table 3. Fractional atomic coordinates, equivalent isotropic displacement parameters and site occupation probabilities (*s.o.p.)* for $La_{20.667}Si_{18}P_{46}Te_{11.333}$.

Atom	Wyckoff Site	*s.o.p.*	*x/a*	*y/b*	*z/c*	U_{eq}/pm^2
La1	4*f*		$^2/_3$	$^1/_3$	0.13122(5)	248(2)
La2	6*h*	0.78(2)$^{a)}$	0.0948(6)	0.5054(6)	$^1/_4$	169(7)
La3	12*i*		0.24402(5)	0.16205(5)	0.13168(3)	203(1)
P5$^{b)}$	4*f*		$^1/_3$	$^2/_3$	0.13792(19)	122(6)
Si2	6*g*		0.4547(3)	0	0	115(6)
Si3	12*i*		0.2609(2)	0.4680(2)	0.08495(12)	128(4)
P1	6*h*		0.2307(3)	0.3504(3)	$^1/_4$	127(6)
P2	12*i*		0.4464(2)	0.1773(2)	0.02724(12)	141(4)
P3	12*i*		0.4311(2)	0.4437(2)	0.10076(12)	146(4)
P4	12*i*		0.1065(2)	0.3111(2)	0.15215(12)	132(4)
Te1	2*a*		0	0	0	261(3)
Te2	2*b*		0	0	$^1/_4$	131(2)
Te3	6*h*		0.44731(11)	0.19065(11)	$^1/_4$	312(2)
Te4$^{c)}$	6*h*	0.22(2)$^{a)}$	0.0432(9)	0.4773(9)	$^1/_4$	112(19)

a) constrained to secure an overall full occupancy according to $0.78+0.22=1.00$ after summation; b) replacing Si1 in Table 2; c) new entry as compared to Table 2, competing with the La2 position.

332.6 pm, 2×). $(La3)^{3+}$ has a coordination number of *C.N.* = 8 accommodating three Te^{2-} anions and five phosphorus atoms in a trigonal dodecahedral shape (d(La3–P) = 301.1–318.4 pm, 5×; d(La3–Te) = 312.4–352.3 pm, 3×; Table 4).

The anionic $^3_\infty\{[Si_{11}P_{21}]^{23-}\}$ sublattice of $La_{11}Si_{11}P_{21}Te_5$ consists of a covalently linked phosphorus-silicon network, which is arranged between the $^1_\infty\{[Te1(La3)^f_{6/2}Te2(La3)^f_{6/2}]^{16+}\}$ columns (Figure 5). This phosphorus-silicon frame comprises tetrahedral $[SiP_4]^{8-}$ and $[Si_2P_3]^{6-}$ building units, which form corrugated layers spreading out parallel to the (001) plane. These are bridged by short $[P_3]^{5-}$ chain fragments (Si3–P4–P1–P4–Si3, d(P–P) = 220–221 pm; Table 4) to complete the three-dimensionality of this mainly covalent substructure (Figure 6). All phosphorus atoms in this structure exhibit only two covalent bonds, which gives them a formal charge of −1 according to the Zintl-Klemm concept, contributing to the overall negative charge of the substructure. P1 assumes a special position in this regard, being the only phosphorus atom, which is not included in a tetrahedral building block of the sublattice. Instead, it serves as a linker between the corrugated $^2_\infty\{[Si_{11}P_{20}]^{22-}\}$ layers (Figure 6).

Silicon occupies three different crystallographic positions. At a closer look, each atom at these sites plays a key role in the present structure. Si1 exhibits only three covalent bonds to other silicon atoms (d(Si1–Si3) = 230.6 pm, 3×), therefore carrying a formal negative charge (−1) and exhibiting an electronic lone pair that seems to take a significant structural responsibility in the compound at hand. It is part of a cage-like structure, which consists of two triplets of corner-sharing $[(Si3)(Si1)P_3]^{6-}$ tetrahedra fused together by $(Si1)^-$ as the common vertex, building a $[Si_4P_9]^{16-}$ subunit, connected by three P1 atoms to a second $[Si_4P_9]^{16-}$ building block. The above-mentioned lone pairs of electrons extend into the cage-like structure and are surrounded by three $(La2)^{3+}$ cations. Si2 resides in the center of a regular $[SiP_4]^{8-}$ tetrahedron (d(Si2–P) = 224.2–224.9 pm, 4×; Table 4) and is the only silicon atom, which does not exhibit a Si–Si bond in this structure. These $[SiP_4]^{8-}$ tetrahedra are acting as linkers between the $[Si_4P_9]^{16-}$ tetrahedral triples and ensure their two-dimensional connection into corrugated layers. Si3 works as the central atom of the above-mentioned tetrahedral $[(Si3)(Si1)P_3]^{6-}$ entities (d(Si3–Si1) = 230.6 pm, 1×; d(Si3–P) = 221.2–224.1 pm, 3×; Table 4), which assemble to the cage-like compartment around the $(La2)^{3+}$ cations.

Figures 7 and 8 give a final view to the crystal structure of $La_{11}Si_{11}P_{21}Te_5$ along the [110] direction emphasizing its division into the two ionic sublattices $^3_\infty\{[La_{11}Te_5]^{23+}\}$ and $^3_\infty\{[Si_{11}P_{21}]^{23-}\}$ in two different ways.

To verify the rough composition of $La_{11}Si_{11}P_{21}Te_5$ and to exclude the possibility of the involvement of other elements, energy-dispersive X-ray spectroscopic (EDXS) measurements on several single crystals at multiple locations on the crystal surfaces were undertaken. The overall summation from these studies suggests a composition like $La_{8.8(5)}Si_{9.9(6)}P_{22(1)}Te_{4.8(6)}$ (19.5(8) mol-% La, 22.0(8) mol-% Si, 49(1) mol-% P, and 10.7(8) mol-% Te) with an over-abundance of the lighter elements in comparison to the single-crystal X-ray diffraction refinement data. From a chemical standpoint, the $(Si1)^-$ anion in the previously described $[(Si1)(Si3)_3]^{6-}$ tripod could indeed be replaced with a neutral phosphorus atom and would not be detectable by means of X-ray diffraction. This is the main difference when comparing the two title compounds with one another. Where the structure of $La_{11}Si_{11}P_{21}Te_5$ can be solved without any residual electron density around the La2 position, the structure of $La_{20.667}Si_{18}P_{46}Te_{11.333}$ seems to be in need of additional electron density in a slightly *off*-position from La2. An erroneously assumed $(La2/\mathit{La4})^{3+}$ split position from the first attempts of structure refinement did not seem to be a satisfactory explanation. Another, and much better, interpretation of the diffraction data for the slightly off-stoichiometric crystal of $La_{20.667}Si_{18}P_{46}Te_{11.333}$ suggests the possibility of a La2/*Te4* split position, in which the $(La2)^{3+}$ vacancy is filled with a

Journal of Inorganic and General Chemistry
ZAAC
Zeitschrift für anorganische und allgemeine Chemie

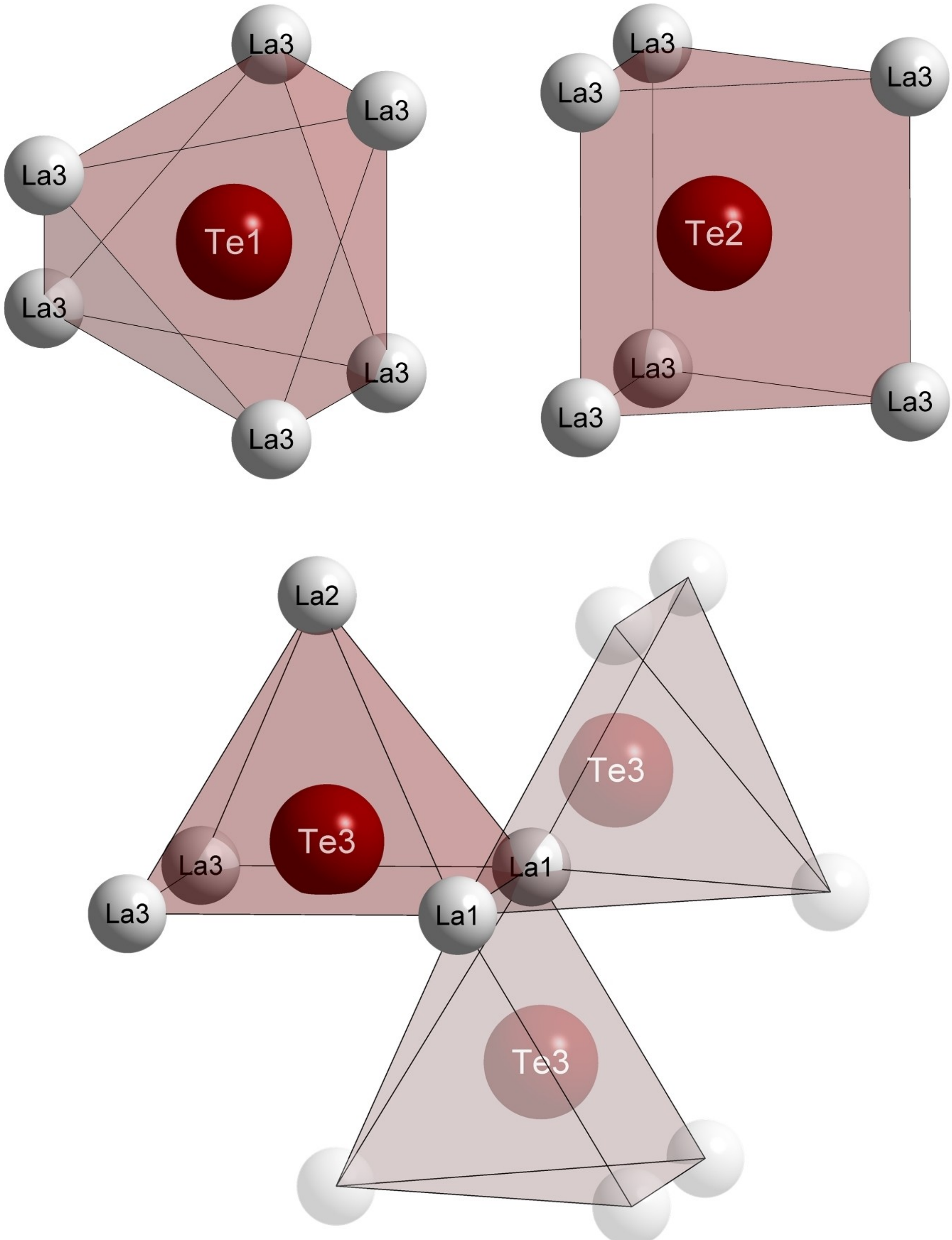

Figure 2. Coordination polyhedra of the Te^{2-} anions in $La_{11}Si_{11}P_{21}Te_5$. Te1 is surrounded by a trigonal hemiprism (top), whereas Te2 centers a trigonal prism of La^{3+} cations (mid). Te3 carries five La^{3+} cations in a square pyramidal fashion and forms a paddle-wheel arrangement with two other $[(Te3)La_5]^{13+}$ polyhedra (bottom).

tellurium atom in forming a (Te3–*Te4*)$^{2-}$ dumbbell, instead of extra (*La4*)$^{3+}$ cations. If just $^4/_3$ La^{3+} cations per doubled empirical formula $La_{22}Si_{22}P_{42}Te_{10}$ are missing, all four (Si1)$^-$ anions need to be replaced with neutral phosphorus atoms (P5) to achieve charge neutrality (Tables 2 and 3). In exchange the missing La^{3+} vacancies at the La2 position need to be filled

Journal of Inorganic and General Chemistry
ZAAC
Zeitschrift für anorganische und allgemeine Chemie

Table 4. Selected interatomic distances (*d*/pm) in $La_{11}Si_{11}P_{21}Te_5$ (left) and $La_{20.667}Si_{18}P_{46}Te_{11.333}$ (right).

Atom pair	Multiplicity	*d*/pm	Atom pair	Multiplicity	*d*/pm
La1–P2	3×	302.8(4)	La1–P2	3×	301.8(2)
La1–Te3	3×	314.3(2)	La1–Te3	3×	316.0(1)
La2–P4	2×	298.1(4)	La2–P4	2×	299.2(3)
La2–P1	1×	304.9(6)	La2–P1	1×	304.0(4)
La2–P3	2×	306.1(4)	La2–P1′	1×	304.3(4)
La2–P1′	1×	307.0(6)	La2–P3	2×	309.2(3)
La2–Te3	1×	314.2(3)	La2–Te3	1×	324.3(7)
La2–Si1	1×	332.6(4)	La2–P5	2×	324.7(6)
La3–P2	1×	301.1(4)	La3–P2	1×	301.4(2)
La3–P4	1×	302.1(4)	La3–P4	1×	301.5(2)
La3–P4′	1×	304.3(4)	La3–P4′	1×	305.1(2)
La3–P3	1×	304.8(4)	La3–P3	1×	304.5(2)
La3–Te3	1×	312.4(2)	La3–Te3	1×	313.5(1)
La3–P1	1×	318.4(4)	La3–P1	1×	317.7(2)
La3–Te2	1×	335.3(1)	La3–Te2	1×	335.8(1)
La3–Te1	1×	352.3(1)	La3–Te1	1×	351.5(1)
Te1–La3	6×	352.3(1)	Te1–La3	6×	351.5(6)
Te2–La3	6×	335.3(1)	Te2–La3	6×	335.8(1)
Te3–La3	2×	312.4(2)	Te3–La3	2×	313.5(1)
Te3–La2	2×	314.2(3)	Te3–La1	2×	316.0(1)
Te3–La1	2×	314.3(2)	Te3–La2	1×	324.3(7)
			Te3–Te4	1×	274.3(9)
Si1–Si3	3×	230.6(5)	P5–Si3	3×	230.6(3)
Si2–P3	2×	224.2(5)	Si2–P3	2×	223.8(3)
Si2–P2	2×	224.9(5)	Si2–P2	2×	224.4(3)
Si3–P2	1×	221.2(5)	Si3–P2	1×	221.6(3)
Si3–P3	1×	222.3(6)	Si3–P3	1×	223.1(3)
Si3–P4	1×	224.1(5)	Si3–P4	1×	223.4(3)
Si3–Si1	1×	230.6(5)	Si3–P5	1×	230.6(3)
P1–P4	2×	220.2(5)	P1–P4	2×	220.6(3)
P2–Si3	1×	221.2(5)	P2–Si3	1×	221.6(3)
P2–Si2	1×	224.9(5)	P2–Si2	1×	224.4(3)
P3–Si3	1×	222.3(6)	P3–Si3	1×	223.1(3)
P3–Si2	1×	224.2(5)	P3–Si2	1×	223.8(3)
P4–P1	1×	220.2(5)	P4–P1	1×	220.6(3)
P4–Si3	1×	224.1(5)	P4–Si3	1×	223.4(3)

with tellurium (*Te4*; *s.o.p.*(La2) + *s.o.p.*(*Te4*) = 0.78(2) + 0.22(2) = 1.00, since nature dislikes to waste space, *d*(La2···*Te4*) = 54 pm), which does not bring any extra charge, as it combines with part of the $(Te3)^{2-}$ anions to form $(Te3–Te4)^{2-}$ dumbbells (*d*(Te3–*Te4*) = 274 pm, Figure 9; other Te···Te distances: *d*(Te3′···*Te4*) = 415 pm or longer) carrying the same double-negative charge. Eventually, this is exactly the new structure description for $La_{20.667}Si_{18}P_{46}Te_{11.333}$ with $Z = 1$ (see Tables 1, 3 and 4), where just one single figure tells the difference with mostly non-bonding interatomic distances like *d*(*Te4*···La2) = 53.9 pm and *d*(*Te4*···P) = 300.0–368.0 pm (8×), as compared to the I_2-analogous homoatomic ditelluride bond of *d*(Te3–*Te4*) = 274.3 pm.

Low-temperature single-crystal X-ray diffraction experiments did not show any increase of order or reduction of symmetry (lattice constants of $La_{20.667}Si_{18}P_{46}Te_{11.333}$: a = 1203.26(5) pm and c = 1798.67(8) pm at 150 K). Nevertheless, the refined partial occupations of the two positions under consideration (0.78 for La2 and 0.22 for Te4) remained the same and in sum exactly 1, which provides a certain reassurance at

Journal of Inorganic and General Chemistry
ZAAC
Zeitschrift für anorganische und allgemeine Chemie

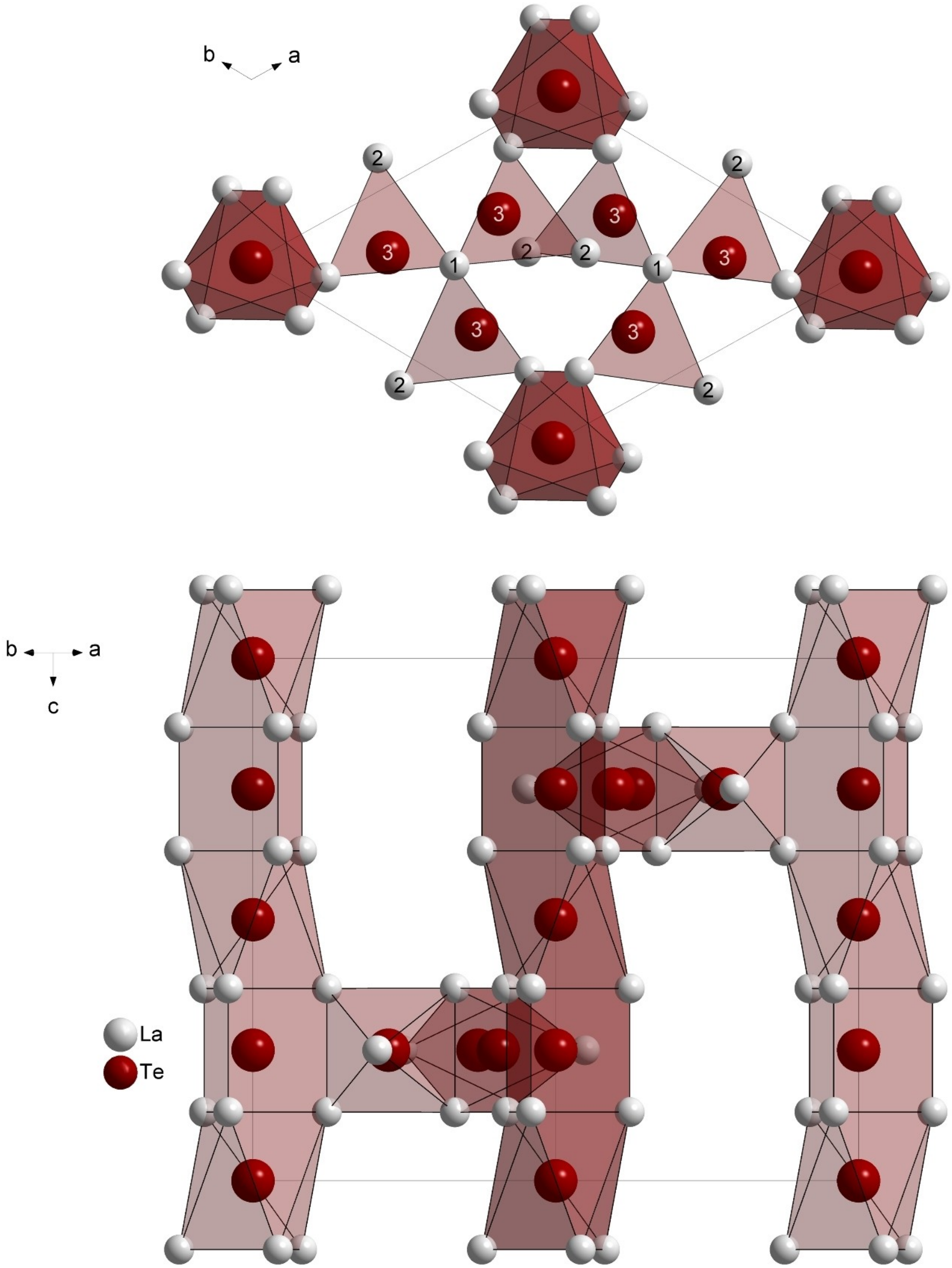

Figure 3. Cationic $^{3}_{\infty}\{[La_{11}Te_5]^{23+}\}$ sublattice in $La_{11}Si_{11}P_{21}Te_5$ with a hexagonal rod-packing (bottom) of infinite $^{1}_{\infty}\{[Te1(La3)^{f}_{6/2}Te2(La3)^{f}_{6/2}]^{16+}\}$ columns running along [001]. The view from above (top) shows the connection of these columns via the paddle wheels of $[(Te3)_3La_{11}]^{27+}$ triples.

least in the light of the crystallographic description of the common overall structure.

Bond-Length Comparisons and Oxidation States

In both title compounds, $La_{11}Si_{11}P_{21}Te_5$ ($Z=2$) and $La_{20.667}Si_{18}P_{46}Te_{11.333}$ ($Z=1$), the La^{3+}–Te^{2-} distances of 314–

335 pm *plus* 352 pm (Table 4) compare well with those in cubic La_2Te_3 (324–342 pm[39,40] or 332–334 pm[41] for *C.N.* = 8) and the same is true for the La–P contacts (298–318 pm), when juxtaposed to those in $LaSiP_3$ (296–330 pm),[32,42] $LaSi_2P_6$ (297–347 pm),[31,43] La_2SiP_4 (293–341 pm)[44] and even LaP (301.3 pm, 6×).[45] The La^{3+}–Si^{-} separations of 333 pm in $La_{11}Si_{11}P_{21}Te_5$ are firstly reported here with this high significance and have no real counterpart in related compounds. In comparison with LaSi (315–331 pm)[46,47] and $LaSi_2$ (316–327 pm),[48] they appear reasonable, however. The Si–Si bond length of 231 pm finds its analogy not only in elemental silicon (235 pm),[49] but also in textbook tables for Si–Si single bonds (234 pm)[38b] and in $Ba_3Si_4P_6$ (236–250 pm)[33] as well. Very similar values for the Si–P bond lengths (221–225 pm) in our new compounds also occur in most phosphidosilicates already quoted in the Introduction[23–33] and many others,[50–55] including the lithium-containing ones[23–25,56,57] pioneered by Thomas F. Fässler, the addressee of our dedication. Moreover, the P–P bond lengths (221–225 pm) mentioned here are common for all phosphorus modifications[38c] with threefold coordinated phosphorus atoms and several polyphosphidosilicates, such as La_2SiP_4,[44] as well as textbook tables for P–P single bonds (222 pm).[38b] Finally, even the Te–Te bond length within the $[Te_2]^{2-}$ dumbbell in $La_{20.667}Si_{18}P_{46}Te_{11.333}$ shows a perfect textbook value of 274 pm[38b] and matches well with these in alkali-metal ditellurides (*e.g.* K_2Te_2: 279 pm[58] and Cs_2Te_2: 278 pm[59]).

Following the scheme of charge distributions (or oxidation states) to the individual atoms of the anionic silicon-phosphorus framework in Table 5, the left column results in 46 negative charges for the ${}^3_\infty\{[Si_{22}P_{42}]^{46-}\}$ case of 2 × $La_{11}Si_{11}P_{21}Te_5$ = $La_{22}Si_{22}P_{42}Te_{10}$ according to $[\{(Si1)^{1-}\}_4\{(Si2)^{4+}\}_6\{(Si3)^{3+}\}_{12}\{(P1)^{1-}\}_6\{(P2)^{3-}\}_{12}\{(P3)^{3-}\}_{12}\{(P4)^{2-}\}_{12}]$, while the right hand column sums up to only 42 of them the case of ${}^3_\infty\{[Si_{18}P_{46}]^{42-}\}$ in $La_{20.667}Si_{18}P_{46}Te_{11.333}$ $([\{(P5)^{0\pm}\}_4\{(Si2)^{4+}\}_6\{(Si3)^{3+}\}_{12}\{(P1)^{1-}\}_6\{(P2)^{3-}\}_{12}\{(P3)^{3-}\}_{12}\{(P4)^{2-}\}_{12}])$. So for $Z = 2$ the anionic network ${}^3_\infty\{[Si_{11}P_{21}]^{23-}\}$

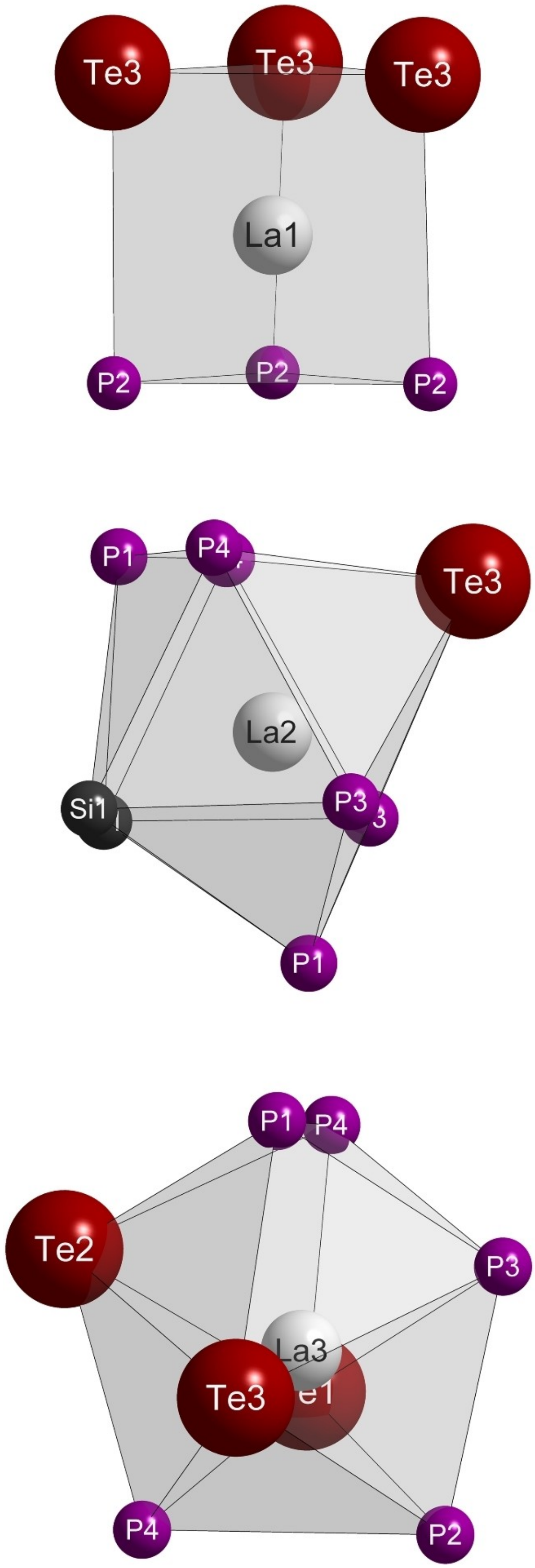

Figure 4. Coordination polyhedra surrounding the La^{3+} cations in $La_{11}Si_{11}P_{21}Te_5$. Trigonal prismatic environment of $(La1)^{3+}$ (top), tricapped trigonal prismatic coordination sphere around $(La2)^{3+}$ (mid) and trigonal dodecahedral surrounding of $(La3)^{3+}$ (bottom).

Table 5. Bonding patterns and charges (oxidation states) of the silicon and phosphorus atoms in the anionic sublattices ${}^3_\infty\{[Si_{11}P_{21}]^{23-}\}$ in $La_{11}Si_{11}P_{21}Te_5$ (left) and ${}^3_\infty\{[Si_{18}P_{46}]^{42-}\}$ in $La_{20.667}Si_{18}P_{46}Te_{11.333}$ (right).

Atom pair	Multiplicity	Charge	Atom pair	Multiplicity	Charge
Si1–Si	3×	Si1: −1	P5–Si	3×	P5: ±0
Si2–P	4×	Si2: +4	Si2–P	4×	Si2: +4
Si3–Si Si3–P	1× 3×	Si3: +3	Si3–P	4×	Si3: +3
P1–P	2×	P1: −1	P1–P	2×	P1: −1
P2–Si	2×	P2: −3	P2–Si	2×	P2: −3
P3–Si	2×	P3: −3	P3–Si	2×	P3: −3
P4–P P4–Si	1× 1×	P4: −2	P4–P P4–Si	1× 1×	P4: −2

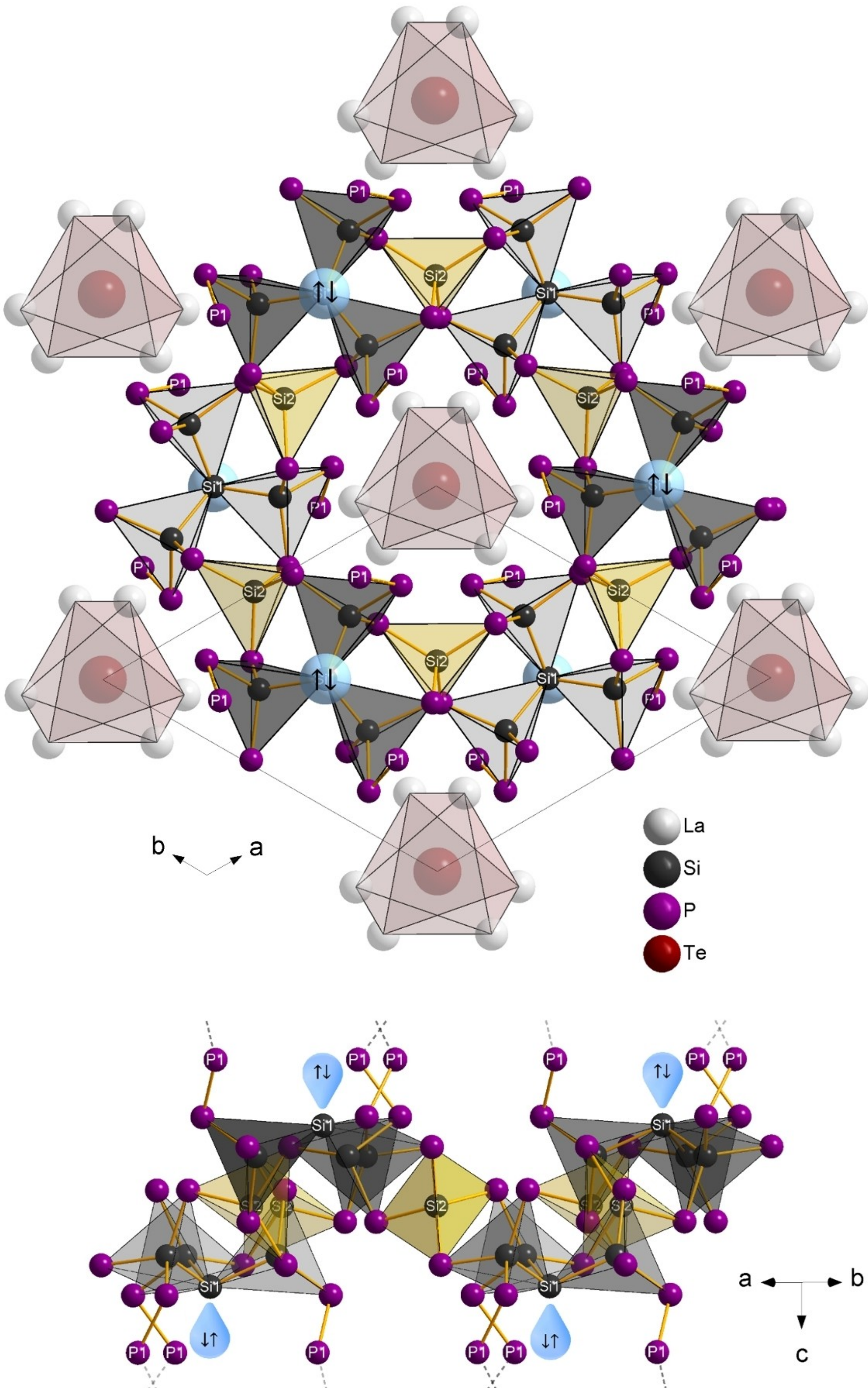

Figure 5. Anionic $^{3}_{\infty}\{[Si_{11}P_{21}]^{23-}\}$ sublattice situated between and around the $^{1}_{\infty}\{[Te1(La3)^{f}_{6/2}Te2(La3)^{f}_{6/2}]^{16+}\}$ columns (top). $[Si_4P_9]^{16-}$ triples of three tetrahedra (gray) connected by $[(Si2)P_4]^{8-}$ tetrahedra (yellow) form corrugated $^{2}_{\infty}\{[Si_{11}P_{20}]^{22-}\}$ layers with electronic lone pairs extending into the voids in between the layers. P1 acts as covalent linker to P4 between the individual sheets (bottom).

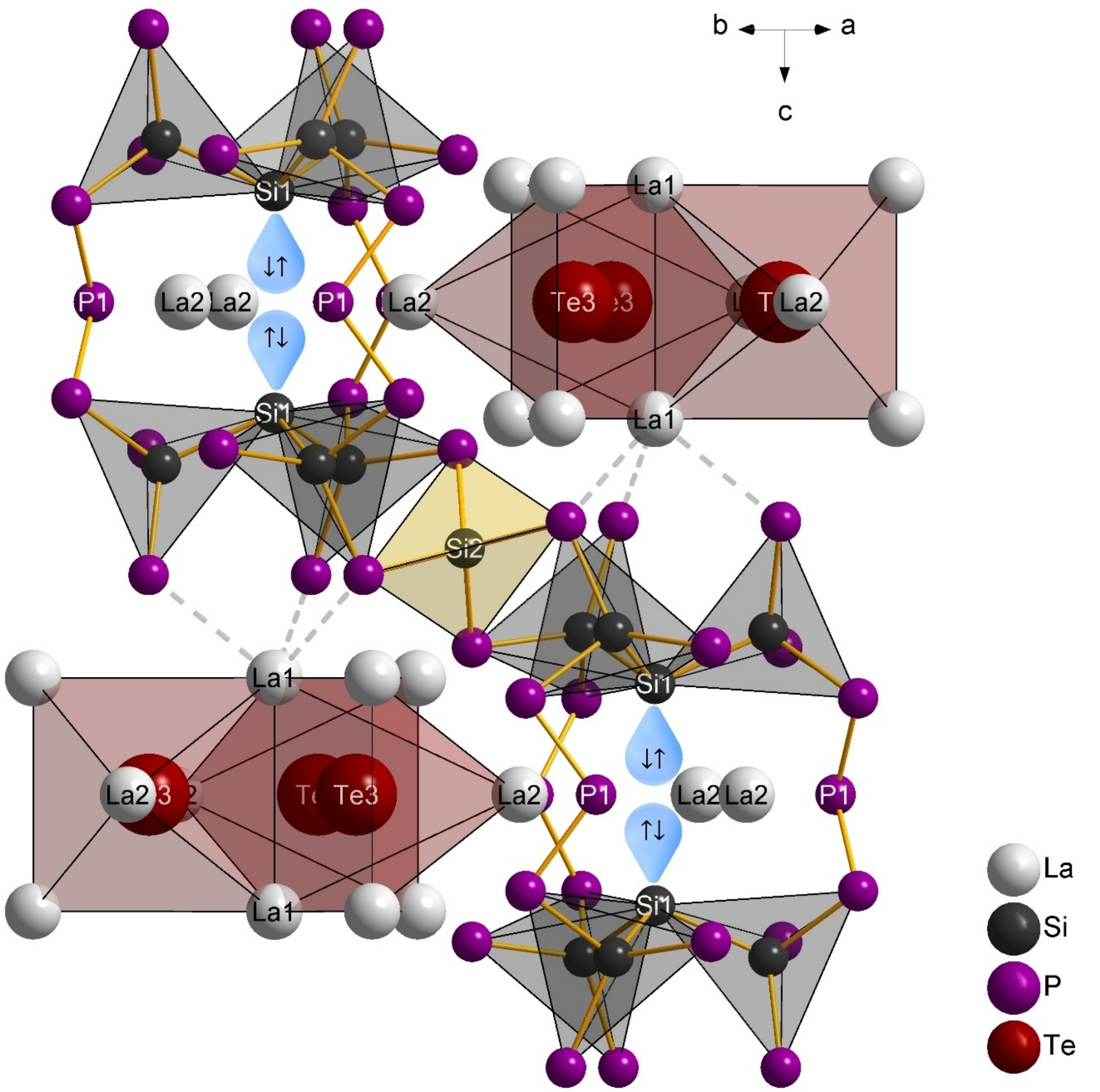

Figure 6. Arrangement of $[Si_4P_9]^{16-}$ tetrahedral triples exhibiting electron lone pairs (shown in blue) provided by the $(Si1)^-$ anions, surrounded by paddle-wheel shaped $[(Te3)_3La_{11}]^{27+}$ triples. The $(La2)^{3+}$ cations are oriented towards the structural void filled by the $(Si1)^-$ lone-pair electrons.

in $La_{11}Si_{11}P_{21}Te_5$ juxtaposes to ${}^3_\infty\{[Si_9P_{23}]^{21-}\}$ in $La_{10.333}Si_9P_{23}Te_{5.667}$, without substantial changes in its structure.

Conclusions

In this work we have presented the so far unknown ternary lanthanum phosphidosilicate tellurides $La_{11}Si_{11}P_{21}Te_5$ and $La_{20.667}Si_{18}P_{46}Te_{11.333}$, which show interesting bonding features between its constituents. One can attribute oxidation states of -1, -2 and -3 to the phosphorus atoms next to -1, $+3$ and $+4$ to silicon in $La_{11}Si_{11}P_{21}Te_5$ alongside the classical "ionic" oxidation states of $+3$ to lanthanum and -2 to tellurium. So this compound should be addressed as lanthanum telluride silicide (poly)phosphidosilicate(III,IV). In the case of $La_{20.667}Si_{18}P_{46}Te_{11.333}$, Si^- gets isomorphously and completely replaced with $P^{0\pm}$, so the silicide component misses. Instead, phosphorus now covers oxidation states ranging from -3 to ± 0 side by side in a single compound, as it is the case for $LaSi_2P_6$.[31] The reduction of the negative charge of the covalently bonded anionic network ${}^3_\infty\{[Si_{11}P_{21}]^{23-}\}$ in $La_{11}Si_{11}P_{21}Te_5$ to ${}^3_\infty\{[Si_9P_{23}]^{21-}\}$ in $La_{10.333}Si_9P_{23}Te_{5.667}$ (both for $Z=2$) forces cationic charge to vanish from 11 La^{3+} cations to 10.333. The resulting vacancy in the cationic substructure ${}^3_\infty\{[La_{11}Te_5]^{23+}\}$ is filled up with tellurium, since nature avoids to waste space, so part of the Te^{2-} anions are transformed into ditelluride dumbbells $[Te_2]^{2-}$ without altering the charge, so that the new formula reads like $La_{10.333}Si_9P_{23}Te_{4.333}[Te_2]_{0.667}$ for $Z=2$ or $La_{20.667}Si_{18}P_{46}Te_{8.667}[Te_2]_{1.333}$ for $Z=1$, also fulfilling the demands of the Zintl-Klemm concept as lanthanum telluride ditelluride

Journal of Inorganic and General Chemistry
ZAAC
Zeitschrift für anorganische und allgemeine Chemie

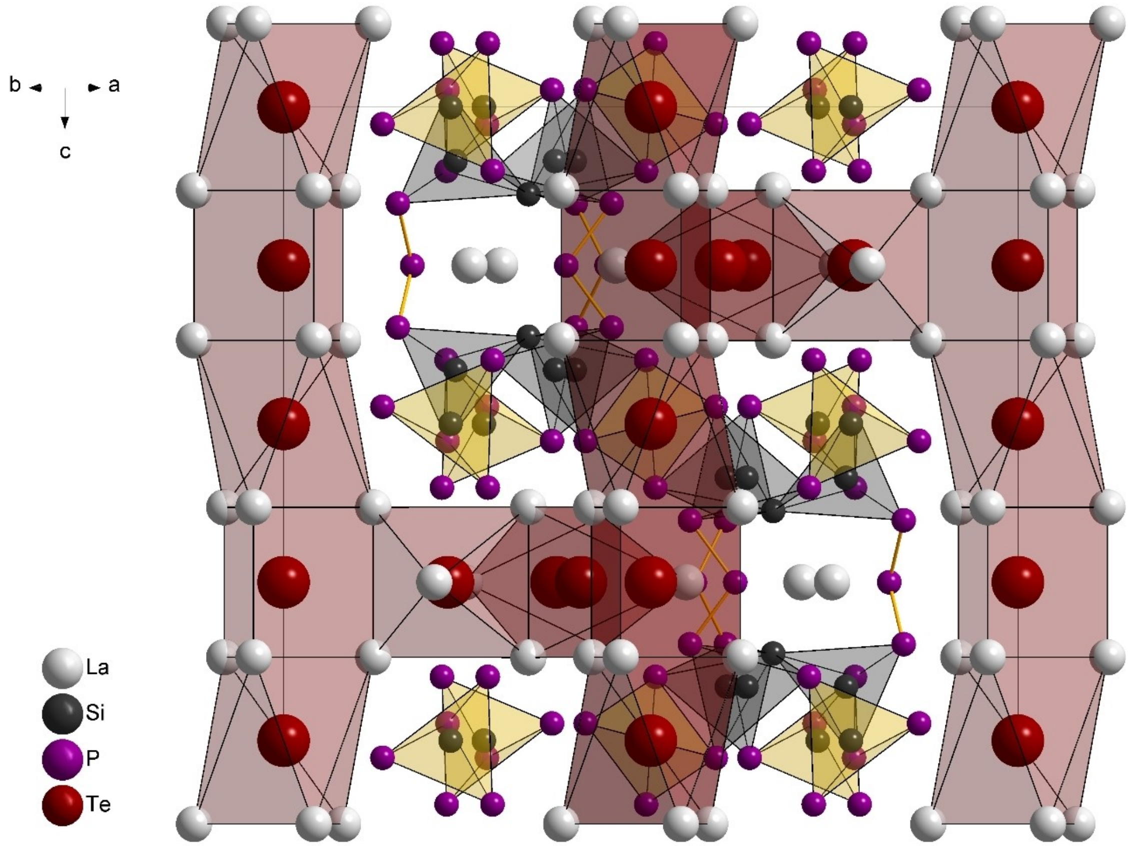

Figure 7. Crystal structure of $La_{11}Si_{11}P_{21}Te_5$ as viewed along [110] with the emphasized division into its sublattices $\{[La_{11}Te_5]^{23+}\}$ and $\{[Si_{11}P_{21}]^{23-}\}$.

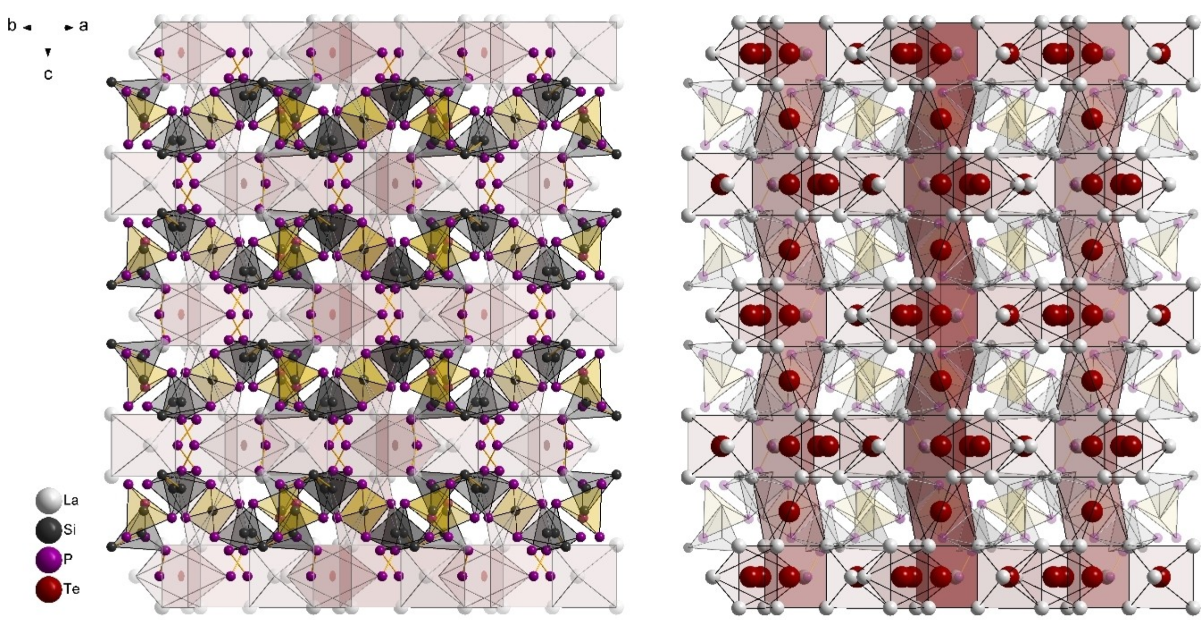

Figure 8. Crystal structure of $La_{11}Si_{11}P_{21}Te_5$ (left: the anionic $\{[Si_{11}P_{21}]^{23-}\}$ sublattice with faded out $\{[La_{11}Te_5]^{23+}\}$ part, right: the cationic $\{[La_{11}Te_5]^{23+}\}$ sublattice with faded out $\{[Si_{11}P_{21}]^{23-}\}$ part) as viewed along [110].

Journal of Inorganic and General Chemistry
ZAAC
Zeitschrift für anorganische und allgemeine Chemie

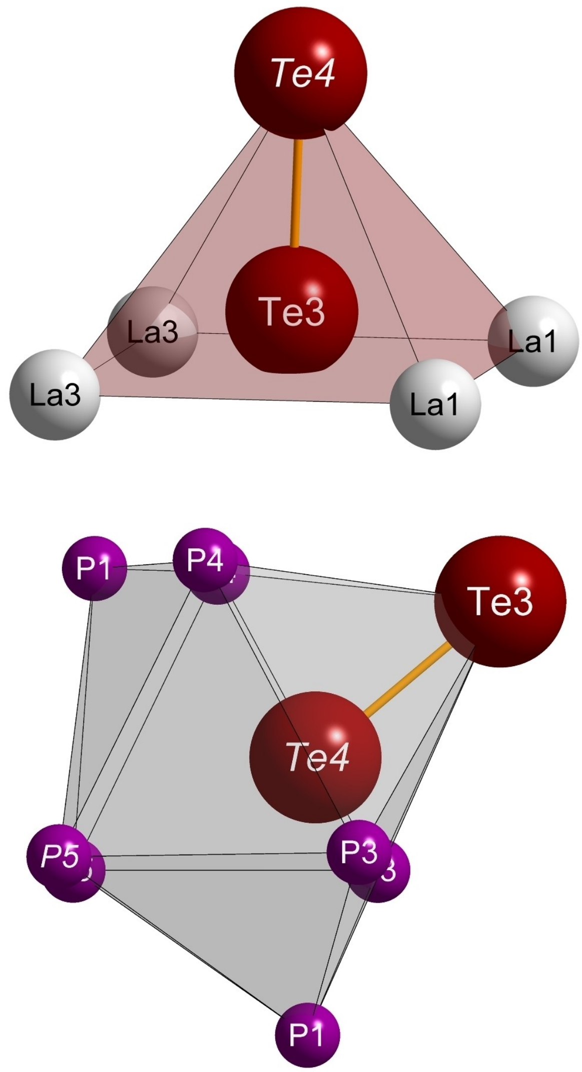

Figure 9. Two polyhedra emphasizing the [(Te3)–(*Te4*)]$^{2-}$ dumbbell as key difference feature between the crystal structures of $La_{11}Si_{11}P_{21}Te_5$ and $La_{20.667}Si_{18}P_{46}Te_{11.333}$, when $(La2)^{3+}$ in $La_{11}Si_{11}P_{21}Te_5$ becomes partly replaced with *Te4* in $La_{20.667}Si_{18}P_{46}Te_{11.333}$.

(poly)phosphidosilicate(IV). Both, $La_{11}Si_{11}P_{21}Te_5$ and $La_{20.667}Si_{18}P_{46}Te_{11.333}$, seem to be stoichiometrically exact "line phases" with a lack of miscibility. Their almost identical lattice constants open the door for the formation of inhomogeneous crystals, however. So the synthesis of real pure phases appears puzzling, but must be a major goal for future research, before further investigations on the thermal and electronic properties of these compounds can be started. First preparative attempts into this direction showed that $La_{11}Si_{11}P_{21}Te_5$ forms best from the elements, since part of the Si–Si bonds from elemental silicon are allowed to persist. The formation of $La_{20.667}Si_{18}P_{46}Te_{11.333}$ seems to be preferred, when SiO_2 serves as silicon source, where no Si–Si bonds occur. Albeit, both compounds give hope to be suitable candidates for thermoelectric applications.

Experimental Section

In an attempt to prepare La_3PTe_3 from the precursors LaP and La_2Te_3 according to

$$\mathrm{LaP} + \mathrm{La_2Te_3} \rightarrow \mathrm{La_3PTe_3} \tag{1}$$

an obviously off-stoichiometry batch with a strong phosphorus surplus[60] must have reacted with SiO_2 of the covering silica tube according to

$$\begin{aligned}&226\ \mathrm{LaP} + 188\ \mathrm{P} + 34\ \mathrm{La_2Te_3} + 162\ \mathrm{SiO_2}\\&\rightarrow 9\ \mathrm{La_{20.667}Si_{18}P_{46}Te_{11.333}} + 54\ \mathrm{La_2O_3}\end{aligned} \tag{2}$$

serendipitously yielding $La_{20.667}Si_{18}P_{46}Te_{11.333}$ along with lanthanum sesquioxide.[61] The latter one has never been detected by PXRD, since as highly basic oxide, La_2O_3 reacts with any acidic oxide around to form ternary compounds, such as detectable monazite-type $La[PO_4]$[62] with P_2O_5 and/or A-type $La_2[Si_2O_7]$[63] with SiO_2. Not only that this reaction could be reproduced successfully with yields of approximately 50 wt.-% by adding external SiO_2 (Merck: silica gel) deliberately, the stoichiometrically exact phase $La_{11}Si_{11}P_{21}Te_5$ could be isolated in a separate experiment by reacting lanthanum metal (La: ChemPur; 99.9 %, 0.55 mmol, 76.4 mg) with silicon powder (Si: Aldrich; 99.999 %, 0.55 mmol, 15.4 mg), red phosphorus powder (P: ChemPur; 99.995 %, 1.05 mmol, 32.5 mg) and tellurium powder (Te: Heraeus; 99.999 %, 0.25 mmol, 31.9 mg) with an excess of potassium chloride (KCl: Merck; 99.9 %, 2.4 mmol, 179 mg) as fluxing agent without further homogenization in evacuated and torch-sealed glassy silica ampoules for four days at 900 °C, applying a heating rate of 37.5 °C·h^{-1}. To prevent phosphorus and tellurium losses during the sealing process of the glassy silica tube, the tube was placed in a liquid nitrogen bath while being evacuated. Ampoule dimensions were selected to maintain a gas pressure of approximately 5 bar at reaction temperatures (around 20 mL ampoule volume). The reaction proceeded as follows:

$$11\ \mathrm{La} + 11\ \mathrm{Si} + 21\ \mathrm{P} + 5\ \mathrm{Te} \rightarrow \mathrm{La_{11}Si_{11}P_{21}Te_5}. \tag{3}$$

Following subsequent cooling at a rate of 12 °C·h^{-1}, the ampoules were cautiously opened within a glove box (GS MEGA E Line, Malsch, Germany) under a dry argon atmosphere. The crude product was then ground in a mortar, and suitable single crystals were selected, while immersed in paraffin oil. Black, semi-metallic lustrous, hexagonally shaped pillars of the title compound (Figure 1) were found among the colorless cubes of the flux salt and selected individually. No other by-products could be identified in this synthesis attempt. One of these crystals were mounted on a κ-CCD four-circle diffractometer (Bruker-Nonius, Karlsruhe, Germany) using graphite-monochromatized Mo-Kα radiation (λ = 71.07 pm) for X-ray diffraction experiments. Structure refinements and solutions were conducted using SHELXL-97[64,65] (scattering factors from International Tables[66]) with a numerical absorption correction obtained from X-SHAPE.[67] A powder X-ray diffraction pattern (Figure 10) was recorded on a STOE Stadi P powder diffractometer (STOE & Cie, Darmstadt, Germany) with Ge(111)-monochromatized Mo-Kα radiation (λ = 71.07 pm) in Debye-Scherrer mode using a Mythen 1 K detector system (Dectris, Baden-Dättwil, Switzerland). The sample was rotated in a glass capillary (diameter: 0.5 mm, Hilgenberg, Malsfeld, Germany) to minimize texture effects. Rietveld refinements[68–70] of the unit-cell parameters with a Pawley fit[71] resulted in a = 1204.9(1) pm and c = 1803.2(2) pm for $La_{11}Si_{11}P_{21}Te_5$ alongside a = 628.7(1) pm for rocksalt-type KCl[72] as second phase. Additionally, semi-quantitative energy-dispersive X-ray spectroscopy (EDXS) measurements were performed on an electron

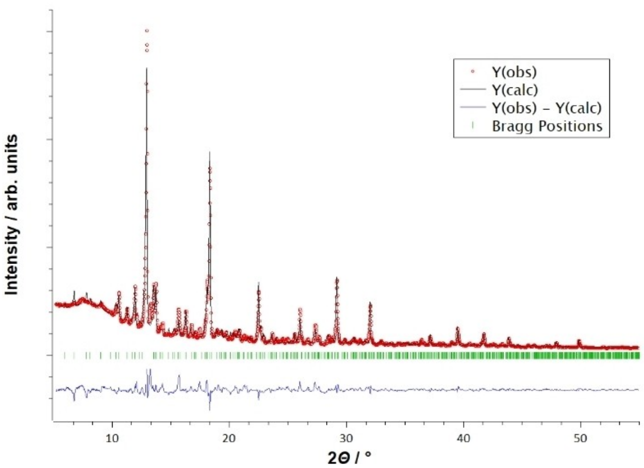

Figure 10. Rietveld refinement of the powder X-ray diffraction data of the product from a mixture designed to produce $La_{11}Si_{11}P_{21}Te_5$ on target after synthesis according to reaction (3) and subsequent grinding.

microscope (Camebax, Cameca, Paris, France) to support the analysis of element distribution in this compound, as silicon and phosphorus can not be distinguished via X-ray diffraction experiments.

Further details of the crystal-structure investigations may be obtained from the Fachinformationszentrum Karlsruhe, 76344 Eggenstein-Leopoldshafen, Germany (Fax: +49-7247-808-666; E-Mail: crysdata@fiz-karlsruhe.de, http://www.fiz-karlsruhe.de/request for deposited data.html), upon quoting the deposition numbers 2361622 for $La_{11}Si_{11}P_{21}Te_5$ and 2351980 for $La_{20.667}Si_{18}P_{46}Te_{11.333}$.

Acknowledgements

The authors gratefully acknowledge Dr. Falk Lissner for the X-ray single-crystal measurements, M.Sc. Yannick Thiebes for the refinement of the powder X-ray diffraction data, M.Sc. Yanina Dreer and M.Sc. Alexandra Friedly for the electron-beam X-ray microanalyses as well as M.Sc. Ralf J. C. Locke for his help during the single-crystal data refinements and depositions. Open Access funding enabled and organized by Projekt DEAL.

Conflict of Interest

The authors declare no conflict of interest.

Data Availability Statement

The data that support the findings of this study are available from the corresponding author upon reasonable request.

Keywords: Lanthanum · Polyphosphides · Phosphidosilicates · Silicides · Tellurides · Crystal structure · Zintl-Klemm concept

[1] W. H. Zachariasen, *Acta Crystallogr.* **1948**, *1*, 265–268.
[2] M. Yarembach, *Colloq. Int. C. N. R. S.* **1970**, *180*, 471–481.
[3] K. Meisel, *Z. Anorg. Allg. Chem.* **1939**, *240*, 300–312.
[4] J. Flahaut, M. Guittard, M. Patrie, M. P. Pardo, S. M. Golabi, L. Domange, *Acta Crystallogr.* **1965**, *19*, 14–19.
[5] N. L. Eatough, A. W. Webb, H. T. Hall, *Inorg. Chem.* **1969**, *8*, 2069–2071.
[6] M. Folchnandt, Th. Schleid, *Z. Anorg. Allg. Chem.* **2001**, *627*, 1411–1413.
[7] P. Djendjur, P. R. Tutsch, Th. Schleid, *Z. Anorg. Allg. Chem.* **2022**, *648*, e202200072 (1–6).
[8] P. Djendjur, N. Atmaca, Th. Schleid, *Acta Crystallogr.* **2022**, *A 78*, e534 (1–2).
[9] E. Zintl, W. Dullenkopf, *Z. Phys. Chem.* **1932**, *B 16*, 183–194.
[10] E. Zintl, G. Brauer, *Z. Phys. Chem.* **1933**, *B 20*, 245–271.
[11] E. Zintl, *Angew. Chem.* **1939**, *52*, 1–48.
[12] W. Klemm, *Z. Anorg. Allg. Chem.* **1941**, *247*, 1–184.
[13] W. Klemm, *Angew. Chem.* **1950**, *62*, 396–402.
[14] W. Klemm, *Angew. Chem.* **1951**, *63*, 133–158.
[15] R. Nesper, *Z. Anorg. Allg. Chem.* **2014**, *640*, 2639–2648.
[16] R. Nesper, H.-G. von Schnering, *J. Solid State Chem.* **1987**, *70*, 48–57.
[17] T. F. Fässler, *Z. Anorg. Allg. Chem.* **2023**, *649*, e202300227 (1–3).
[18] T. Goebel, Y. Prots, F. Haarmann, *Z. Kristallogr. New Cryst. Struct.* **2008**, *223*, 187–188.
[19] H.-G. von Schnering, M. Schwarz, R. Nesper, *J. Less-Common Met.* **1988**, *137*, 297–310.
[20] F. Hulliger, R. Schmelczer, D. Schwarzenbach, *J. Solid State Chem.* **1977**, *21*, 371–374.
[21] P. W. Schenk, *Z. Anorg. Allg. Chem.* **1955**, *280*, 1–23.
[22] P. Cherin, P. Unger, *Inorg. Chem.* **1967**, *6*, 1589–1591.
[23] H. Eickhoff, S. Strangmüller, W. Klein, H. Kirchhain, C. Dietrich, W. G. Zeier, L. van Wüllen, T. F. Fässler, *Chem. Mater.* **2018**, *30*, 6440–6448.
[24] L. Toffoletti, H. Kirchhain, J. Landesfeind, W. Klein, L. van Wüllen, H. A. Gasteiger, T. F. Fässler, *Chem. Eur. J.* **2016**, *22*, 17635–1764.
[25] V. Daiber, S. Zeitz, V. Hlukhyy, D. Dankert, T. F. Fässler, *Z. Anorg. Allg. Chem.* **2024**, *650*, e202300244 (1–8).
[26] A. Haffner, A.-K. Hatz, C. Hoch, B. V. Lotsch, D. Johrendt, *Eur. J. Inorg. Chem.* **2020**, *2020*, 617–621.
[27] K. Feng, L. Kang, W. Yin, W. Hao, Z. Lin, J. Yao, Y. Wu, *J. Solid State Chem.* **2013**, *205*, 129–133.
[28] A. Haffner, T. Bräuniger, D. Johrendt, *Angew. Chem. Int. Ed.* **2016**, *55*, 13585–13588.
[29] A. Haffner, A.-K. Hatz, O. E. O. Zeman, C. Hoch, B. V. Lotsch, D. Johrendt, *Angew. Chem. Int. Ed.* **2021**, *60*, 13641–13646.
[30] A. Haffner, A.-K. Hatz, I. Moudrakovski, B. V. Lotsch, D. Johrendt, *Angew. Chem. Int. Ed.* **2018**, *57*, 6155–6160.
[31] P. Kaiser, W. Jeitschko, *J. Solid State Chem.* **1996**, *124*, 346–352.
[32] Y. Sun, J. Chen, S. Yang, B. Li, G. Chai, C. Lin, M. Luo, N. Ye, *Adv. Opt. Mater.* **2021**, *9*, 2002176 (1–9).
[33] B. Eisenmann, H. Jordan, H. Schäfer, *Z. Naturforsch.* **1984**, *39b*, 864–867.
[34] H. D. Flack, *Acta Crystallogr.* **1983**, *A39*, 876–881.
[35] L. Pauling, *J. Am. Chem. Soc.* **1932**, *54*, 3570–3582.
[36] L. Pauling, *The Nature of the Chemical Bond and the Structure of Molecules and Crystals: An Introduction to Modern Structural Chemistry*, Cornell University Press, 2nd Ed., Ithaca, NY, USA **1940**.
[37] A. L. Allred, E. G. Rochow, *J. Inorg. Nucl. Chem.* **1958**, *5*, 264–268.
[38] A. F. Holleman, E. Wiberg, *Lehrbuch der Anorganischen Chemie*, Verlag Walter de Gruyter, 81.–90. Aufl., Berlin, New York **1976**; a) p. 123 (Elektronegativitäten); b) p. 129 (Einfachbindungslängen); c) p. 425–429 (Phosphormodifikationen).

[39] W. L. Mularz, S. J. Wolnik, *Proc. Conf. Rare Earth Res.* **1963/64**, *3*, 473–479.
[40] V. V. Sokolov, L. K. Kravchenko, A. A. Kamarzin, *Inorg. Mater.* **1973**, *9*, 944–946.
[41] D. J. Haase, H. Steinfink, E. J. Weiss, *Proc. Conf. Rare Earth Res.* **1964/65**, *4*, 535–544.
[42] G. Akopov, J. Mark, G. Viswanathan, S. J. Lee, B. C. McBride, J. Won, F. A. Perras, A. L. Paterson, B. Yuan, S. Sen, A. N. Adeyemi, F. Zhang, C.-Z. Wang, K.-M. Ho, G. J. Miller, K. Kovnir, *Dalton Trans.* **2021**, *50*, 6463–6476.
[43] S. Ono, H. Hayakawa, K. Nomura, *Nippon Kagaku Kaishi* **1976**, *5*, 1700–1709.
[44] G. Akopov, G. Viswanathan, K. Kovnir, *Z. Anorg. Allg. Chem.* **2021**, *647*, 91–97.
[45] S. Ono, K. Nomura, H. Hayakawa, *J. Less-Common Met.* **1974**, *38*, 119–130.
[46] A. Raman, H. Steinfink, *Acta Crystallogr.* **1967**, *22*, 688–691.
[47] D. Hohnke, E. Parthé, *Acta Crystallogr.* **1966**, *20*, 572–582.
[48] A. Raman, H. Steinfink, *Inorg. Chem.* **1967**, *6*, 1789–1791.
[49] D. M. Többens, N. Stüßer, K. Knorr, H. M. Mayer, *Mater. Sci. Forum* **2001**, *378*, 288–293.
[50] B. Eisenmann, H. Jordan, H. Schäfer, *Mater. Res. Bull.* **1984**, *17*, 95–99.
[51] B. Eisenmann, J. Klein, *J. Less-Common Met.* **1991**, *175*, 109–117.
[52] K. Feng, L. Kang, W. Yin, W. Hao, Z. Lin, J. Yao, Y. Wu, *J. Solid State Chem.* **2013**, *205*, 129–133.
[53] J. Mark, J.-A. Dolyniuk, N. Tran, K. Kovnir, *Z. Anorg. Allg. Chem.* **2019**, *645*, 242–247.
[54] J. Mark, J. Wang, K. Wu, J. G. Lo, S. Lee, K. Kovnir, *J. Am. Chem. Soc.* **2019**, *141*, 11976–11983.
[55] A. Haffner, V. Weippert, D. Johrendt, *Z. Anorg. Allg. Chem.* **2021**, *647*, 326–330.
[56] H. Eickhoff, L. Toffoletti, W. Klein, G. Raudaschl-Sieber, T. F. Fässler, *Inorg. Chem.* **2017**, *56*, 6688–6694.
[57] S. Strangmüller, H. Eickhoff, D. Müller, W. Klein, G. Raudaschl-Sieber, H. Kirchhain, C. Sedlmeier, V. Baran, A. Senyshyn, V. L. Deringer, L. van Wüllen, H. A. Gasteiger, T. F. Fässler, *J. Am. Chem. Soc.* **2019**, *141*, 14200–14209.
[58] P. Böttcher, J. Getzschmann, R. Keller, *Z. Anorg. Allg. Chem.* **1993**, *619*, 476–488.
[59] J. Getzschmann, P. Böttcher, W. Kaluza, *Z. Kristallogr.* **1996**, *211*, 90–95.
[60] Z. A. Anschütz, *Bachelor Thesis*, University of Stuttgart, **2022**.
[61] W. C. Koehler, E. O. Wollan, *Acta Crystallogr.* **1953**, *6*, 741–742.
[62] Y.-X. Ni, J. M. Hughes, A. N. Mariano, *Am. Mineral.* **1995**, *80*, 21–26.
[63] H. Müller-Bunz, Th. Schleid, *Z. Anorg. Allg. Chem.* **2000**, *626*, 2549–2556.
[64] G. M. Sheldrick, *Programmpaket SHELX-97*, Universität Göttingen, Göttingen **1997**.
[65] G. M. Sheldrick, *Acta Crystallogr.* **2007**, *A64*, 112–122.
[66] *International Tables for Crystallography, Vol. C* (Ed.: E. Prince), 3. Auflage, Springer-Verlag, Dordrecht **2004**.
[67] W. Herrendorf, H. Bärnighausen, *HABITUS (Version 1.06). A Program for the Optimization of the Crystal Shape for Numerical Absorption Correction in X-SHAPE*, Stoe, Darmstadt, Karlsruhe, Germany **1996/97**.
[68] H. M. Rietveld, *Acta Crystallogr.* **1967**, *22*, 151–152.
[69] H. M. Rietveld, *J. Appl. Crystallogr.* **1969**, *2*, 65–71.
[70] H. M. Rietveld, *Z. Kristallogr.* **2010**, *225*, 545–547.
[71] J. Rodríguez-Carvajal, *Programm FullProf.2k, Version 5.30*, Grenoble, France **2012**.
[72] H. Ott, *Z. Kristallogr.* **1926**, *63*, 222–230.

Manuscript received: June 26, 2024
Revised manuscript received: August 15, 2024